INFLUENCE OF THE MEAN LOAD EFFECT INTERPRETATION ON THE FATIGUE LIFE PREDICTION OF GFRP STRUCTURAL JOINTS

Roohollah Sarfaraz, Anastasios P. Vassilopoulos*, Thomas Keller

Composite Construction Laboratory (CCLab), Ecole Polytechnique Fédérale de Lausanne (EPFL), Station 16, Bâtiment BP, CH-1015 Lausanne, Switzerland
**e-mail address: anastasios.vasilopoulos@epfl.ch*

Keywords: Bonded joints, pultruded GFRP, constant life diagram, variable amplitude fatigue.

Abstract

In previous papers by the authors and other researchers it has been proved that, although the classic linear Goodman diagram is the most commonly used, particularly for metals, it is not suitable for composite materials and composite structural components, mainly because of the variation in their tensile and compressive strengths and the different tensile and compressive failure modes that they exhibit. As a result, a typical constant life diagram (CLD) for composite materials or structural components is shifted, and the highest point is located away from the line corresponding to zero mean stress, $\sigma_m=0$*, or else the line representing the reversed S–N curve with a ratio between the minimum and maximum applied stress, R= –1. Therefore, straight lines connecting the ultimate tensile stress (UTS) and the ultimate compressive stress (UCS) with points on the R= –1 line for different numbers of cycles are not capable of describing the real fatigue behavior of composite materials. To cope with these various characteristics of composite materials and composite structural elements, several different models have been presented in the literature. This paper examines the influence of the constant life diagram formulation selection on the prediction of the fatigue life of adhesively bonded GFRP structural joints. The most commonly used and most recent CLD formulations for composite materials and joints are evaluated.*

1 Introduction

The influence of the *R*-ratio (the ratio of the minimum to the maximum applied cyclic load) on the fatigue behavior of composite materials has been the subject of numerous investigations in the past, e.g. [1, 2]. This effect is assessed by using constant life diagrams (CLD). Constant life diagrams reflect the combined effect of mean stress and material anisotropy on fatigue life, and can be used for estimation of the fatigue life of the material under loading patterns for which no experimental data exist. The main parameters that define a CLD are the cyclic mean stress, stress amplitude and number of fatigue cycles. The CLDs for composite materials are usually shifted towards the tension- or compression-dominated domain, reflecting the degree of anisotropy of the examined material [3, 4]. For laminates exhibiting significantly higher tensile strength than compressive strength, e.g. unidirectional carbon/epoxy laminates [3], the CLD is shifted towards the right, tension-dominated domain. For materials exhibiting higher compressive than tensile fatigue properties, e.g. short- fiber composites [5], the diagram is shifted towards the compression-dominated domain. It has also been reported that this tendency towards one side of the diagram can alter with the number of cycles. A change in the form of the iso-life curves was also reported in [3, 6]. The shape of the curves gradually alters from linear to non-linear form with increasing fatigue life.

The classic CLD formulations require that the constant life lines converge to the ultimate tensile stress (UTS) and the ultimate compressive stress (UCS), regardless of the number of loading cycles [4]. However, this is an arbitrary simplification originating from the lack of information about the fatigue behavior of the material when no amplitude is applied. In fact, this type of loading cannot be considered as fatigue loading, but rather as creep of the material (constant static load over a short or long period), see e.g. [7]. Although modifications to take the time-dependent material strength into account have been introduced, their integration into CLD formulations requires the adoption of additional assumptions, see e.g. [8], and yet none of these modifications can provide a general model to characterize the fatigue-creep interaction in composite materials.

Although a considerable amount of information exists regarding the *R*-ratio effect on the fatigue life of composite laminates, there is little literature regarding similar investigations for adhesively-bonded structural joints. Experimental studies on joints are based on tensile fatigue loads because they focus on joints exhibiting a cohesive or an adhesive failure. Nevertheless, as shown from several studies, different failure modes can be observed depending on the adherend materials and the joint geometry. Moreover, significant *R*-ratio effects were reported, e.g. [9], especially for pultruded FRP joints in which cracks in the adherend lead the failure process and also different failure modes are observed under tension and compression fatigue [10].

The effect of a combination of tensile and compressive loads on the fatigue behavior of adhesively-bonded pultruded GFRP joints has been studied in the present work by generating load-life data for a range of *R*-ratios covering all CLD domains. The constant life behavior of the examined joints is modeled by several different CLD formulations. The influence of the CLD formulation selection on the prediction of the fatigue life of adhesively bonded GFRP structural joints is finally investigated. The effect of the selection of the CLD formulation on variable amplitude fatigue life prediction is assessed according to the life prediction results, although other parameters that influence the results (S-N curve type, damage summation rule, etc.) may mask the effect of the CLD formulation. Fatigue data from adhesively bonded GFRP structural joints are used for the demonstration. Based on the results, recommendations concerning the applicability, advantages and disadvantages of each of the examined CLD formulations are extensively discussed.

2 Experimental investigation

2.1 Experimental program

Symmetric adhesively-bonded double-lap joints composed of pultruded GFRP laminates bonded by an epoxy adhesive system were examined under axial, tensile, compressive and reversed fatigue loads. The pultruded GFRP laminates, supplied by Fiberline A/S, Denmark, consisted of E-glass fibers and isophthalic polyester resin. The laminates comprised two mat layers on each side and a roving layer in the middle with a thin layer of polyester veil on the outer surfaces. Each mat layer comprised of 0/90 woven fabric stitched to a chopped strand mat (CSM). A two-component epoxy adhesive system was used (Sikadur 330, Sika AG, Switzerland) as the bonding material [10].

Two different joint configurations were prepared; one with a total length of 410 mm, see Fig. 1, and used only for tensile loading, and another with a reduced total length of 350 mm, which was used when compressive loads were applied to avoid any buckling of the joints. To achieve the latter configuration, the free length of the “inner laminate” was reduced from 100 mm to 40 mm without changing the bonding and gripping length. These dimensions were selected after preliminary testing and modal analysis using finite element modeling, which indicated that this length reduction sufficed to prevent buckling of the laminates. Furthermore, the finite element stress analysis showed that this change of the laminate length did not result in significant changes in all stress components, through the inner laminate and the bonding area thickness, and also in the interface along the bond line. The gripping part (shown on the right side of Fig. 1) was designed to adapt the thickness of the specimen to the jaw faces of the machine. A bolted connection was used to prevent any failure in the gripping part that may have affected joint behavior. All fatigue experiments were carried out on an INSTRON 8800 servohydraulic machine under laboratory conditions (23±5°C and 50±10% RH) under load control, using a constant amplitude sinusoidal waveform, and a frequency of 10 Hz. Six *R*-ratios were selected to cover as many CLD domains as possible; *R*= 0.5 and *R*= 0.9 for the tension-tension (T-T) domain, *R*= 2 and *R*= 1.1 for the compression-compression (C-C) domain, *R*= –0.5 for the tension dominated-compression (T-C) domain, and *R*= –2 for the compression dominated-tension (C-T) domain. At least six specimens were examined under each R-ratio in order to cover the entire lifetime between low and high cycle fatigue. The experimental results of this work complement a previously derived database containing fatigue data from experiments on the same joint type under *R*= 0.1, 10, and –1, [10].

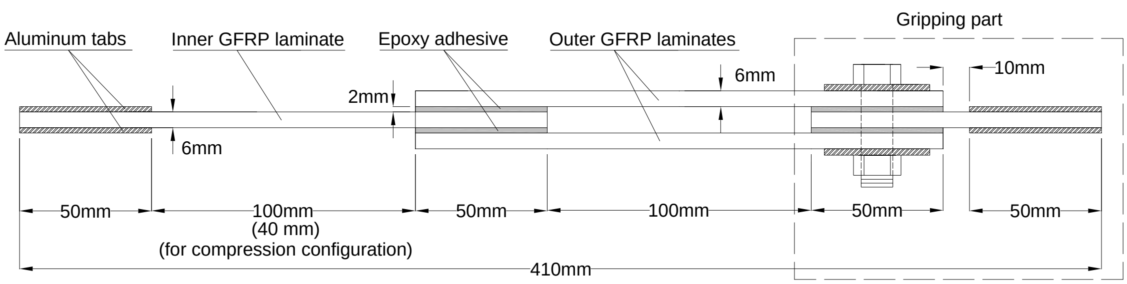

Figure 1. Double-lap joint geometry

2.2 Experimental results

Under T-T (*R*= 0.5 and *R*= 0.9) and T-C (*R*= –0.5) fatigue, the failure mode was similar to that observed under T-T (*R*= 0.1). A fiber-tear failure was observed with a dominant crack that initiated from the joint corner of one of the bond lines, between the adhesive and the inner GFRP laminate, and then shifted deeper, between the first and the second mat layers of the inner laminate, and propagated along this path up to failure. Under C-C loading (*R*= 2 and *R*= 1.1), as under *R*= 10, failure occurred within the roving layer of the inner laminate. Under C-T loading (*R*= –2), the failure mode was similar to *R*= –1, as reported in [10]. Under this loading condition, in addition to the dominant crack along one of the bond lines related to the tensile component of loading, a smaller crack was observed in the middle of the inner laminate at a similar location as for compression fatigue. However, during the fatigue life the dominant crack was propagating and leading the failure process, while the crack created by the compressive component of the applied cyclic load reached a maximum length of 5 mm prior to the failure of the joint. These observations showed that the failure transition occurred beyond the load ratio *R*= –1 in the C-T region, which is consistent with the higher fatigue strength of joints under compressive loading, see [10].

2.3. Fatigue life

The experimental program was designed and maximum load levels were applied in order to obtain representative experimental data in the range between 1 and 10^8 cycles. The fatigue life of the examined joints under the applied *R*-ratios is plotted against the cyclic load amplitude in Figs. 2a and 2b for the experiments under positive and negative mean loads respectively.

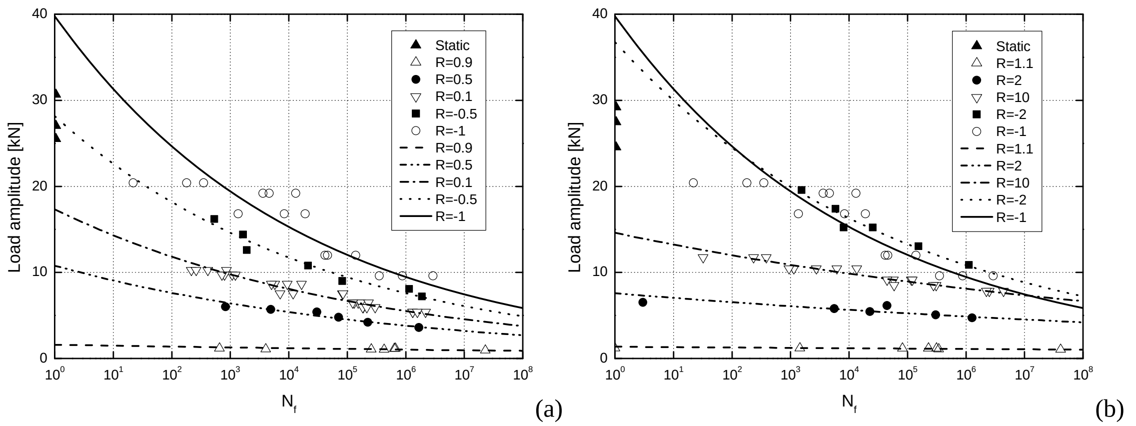

Figure 2. S-N data for T-T and T-C fatigue loading (2a) and for C-C and C-T fatigue loading (2b)

The S-N curve for *R*=–1 exhibits the highest slope, demonstrating the sensitivity of the examined joints to reversed loading. As shown in Figs. 2a and 2b, the fatigue strength of joints decreases under higher *R*-ratios at tensile and tensile-dominated loading. In contrast it decreases under lower *R*-ratios at compression and compression-dominated loading. Under high mean loads (e.g. *R*=0.9 and *R*=1.1), close to the static strength of the joints, the fatigue life is very sensitive to the change of load amplitude and S-N curves become flatter with lower slopes.

However, one exception to this rule is observed when the mean load is decreased from zero, *R*= –1, to a negative level, i.e. *R*= –2. The S-N data for *R*= –2 in Fig. 2b is located slightly higher than the fatigue data for *R*= –1. As already explained, although the compressive part of the cyclic load was dominant at this *R*-ratio, the observed failure mode, similar to the reverse loading (*R*= –1), was tensile failure. This behavior occurs due to the higher fatigue strength of the examined joints under compression fatigue. Compared to *R*= –1, a higher load amplitude is required to reach the same maximum load level under *R*= –2. Therefore the highest load amplitude occurs at a load ratio other than *R*= –1 i.e. under a C-T loading condition where a transition in failure occurs from tensile to compressive mode.

2.2.3. Constant life diagram

The effect of load ratio on the fatigue life of the examined joints can also be visualized by using constant life diagrams. For the derivation of a CLD, the fatigue data are normally (although not necessarily, see [11]) plotted on the "mean-amplitude" (σ_m-σ_a) plane, as radial lines emanating from the origin of the coordinate system. Each radial line represents a single S-N curve under a given *R*-ratio and can be reproduced using the following equation:

$$\sigma_a = \left(\frac{1-R}{1+R}\right)\sigma_m \qquad (2)$$

Constant life diagrams are formed by joining in a linear or non-linear way the points (creating iso-life curves) corresponding to the same number of cycles on consecutive radial lines.

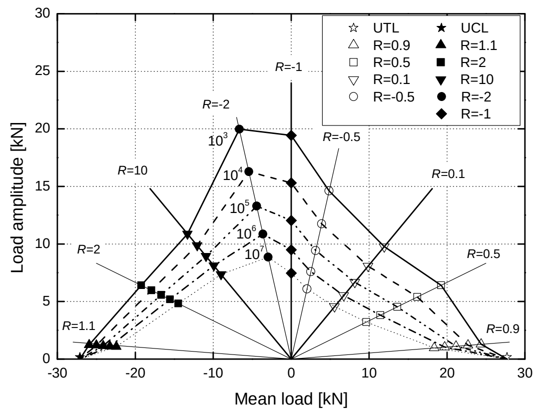

Figure 3. Variation of alternating load vs. mean load at different fatigue lives

The constant life diagram for the examined joint configuration is shown in Fig. 3. It is obvious that the CLD is not symmetric with respect to the zero mean cyclic load axis and shifted somewhat towards the compression-dominated domain with the apex corresponding to the S-N curve under *R*= –2. This behavior can be attributed to the difference in fatigue strength under tension and compression loading as discussed above. An inflection in the curvature of the iso-life curves is observed, as they change from concave to convex when the loading condition shifts from T-T or C-C to combined tension-compression fatigue loading. Moreover it is observed that the ultimate tensile and compressive load (UTL=27.7±2.17 kN and UCL=–27.1±1.92 kN) values are not appropriate for description of the fatigue behavior under zero load amplitude since, as shown in Fig. 3, a fatigue-creep interaction occurs under *R*-ratios close to 1 due to the presence of very low amplitude and high mean values that characterize the cyclic loading in this region.

4. Results and discussion

The linear (LR) [4], the piecewise non-linear (PNL) [11], the Boerstra (BR) [4] and the polynomial formulations (POLY) [12] were selected for the modeling of the *R*-ratio effect on the fatigue life of the examined joints. The constant life diagrams produced by the described models are shown in Figs. 4 and 5.

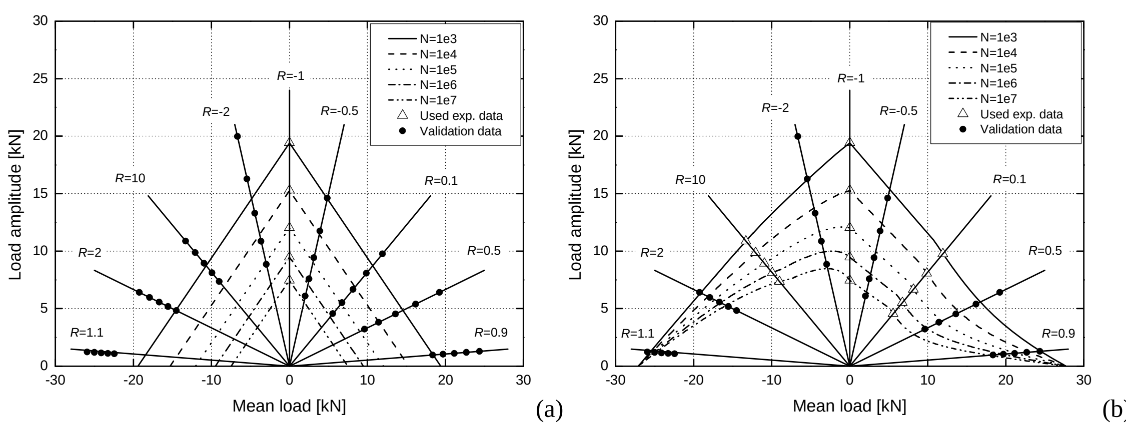

Figure 4. Linear (a) and Piecewise non-linear (b) constant life diagrams

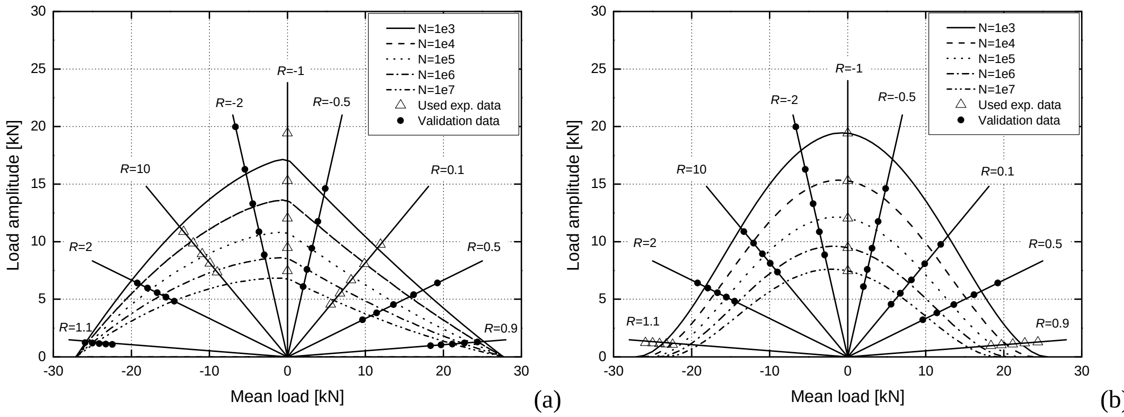

Figure 5. Boerstra's (a) and Polynomial (b) constant life diagrams

Data used for the estimation of model parameters are shown by open triangles, while data used for the model validation are shown by closed circles in all figures. A quantification of the predictive ability of each of the applied models was performed.

The linear model shown in Fig. 4(a), using only fatigue data at *R*= –1, underestimates the fatigue life in all regions except for *R*= –0.5. The PNL formulation, can appropriately describe the concave upward behavior in the region between *R*= 1 and *R*= 0.1 (see Fig. 4(b)). In this case, the shift of the apex of the iso-life curves toward the negative mean load quadrant at a high number of cycles improves modeling accuracy. On the other hand, the convex shape of the curves between *R*= 10 and *R*= 1 reduces its accuracy. The use of five parameters for the derivation of the BR constant life diagram makes it very flexible and able to accurately model the fatigue behavior of a large number of different material systems (Fig. 5(a)). The average accuracy of Boerstra's CLD (R^2=0.748) is one of the highest among the examined models. Nonetheless, the fatigue life in regions susceptible to creep is overestimated. Also, since the model parameters are calculated based on an optimization process, the CLD only satisfies the boundary conditions at zero load amplitude. Consequently the iso-life lines do not necessarily comply with the experimental data employed for modeling, as shown in Fig. 5(a). The polynomial constant life diagram presented in Fig. 5(b) shows the capability of this CLD model to follow the trend of the experimental data. It is apparent that incorporating the creep rupture strength data (actually the fatigue data under *R*= 0.9 (T-T) and *R*= 1.1 (C-C)) into the formulation, instead of using the static strength values, improves the accuracy of the model predictions in high mean load regions. Although under the applied boundary conditions the constant life lines must satisfy the fatigue failure condition under reversed loading (when $\sigma_m = 0,\ \sigma_a = \sigma_{(R=-1)}$), this does not impose a maximum value of the CLD on the radial line representing the S-N curve under *R*= –1. The model allows the diagram to move towards the tension- or compression-dominated domain according to the experimental evidence. The highest average R^2 value with the lowest standard deviation obtained for the new CLD formulation, 0.775±0.196, proved the good accuracy and consistency of the model.

2.2.3. Life prediction

The predictive accuracy of the applied CLD models was evaluated by comparing predicted S-N curves with corresponding experimental ones that were not used for estimation of the model parameters.

To quantify the result, predicted S-N curves from the different models are presented in Fig. 6 and compared to the available experimental data for arbitrarily selected cases. As shown, the linear model underestimates the fatigue strength of the examined material in all the examined cases, leading to conservative fatigue life predictions. On the other hand, the three remaining models are quite accurate in both cases. It has to be mentioned that the modeling accuracy depends on the quality of the examined fatigue data, the selected input data (e.g. for the linear model) and the quality of the fitting and/or optimization for estimation of the parameters (e.g., the BR model).

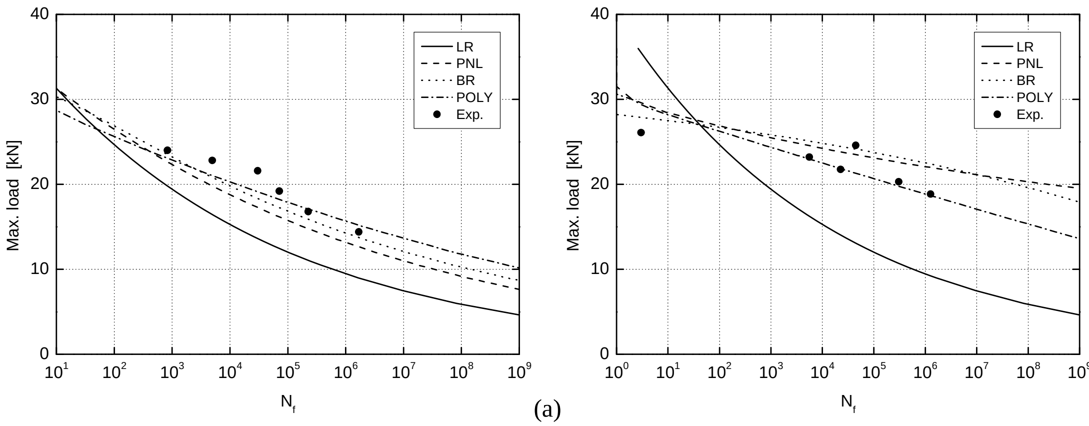

Figure 6. Constant amplitude life prediction for T-T fatigue (*R*=0.5) (a) and C-C fatigue (*R*=2) (b).

Although some of the used CLD models provide similar S-N curve predictions for specific *R*-ratios (as shown in Fig. 6) this is not consistent. Therefore the offered predictions for the life under variable amplitude fatigue spectra can be significantly different as shown in Fig. 7. The degree of accuracy depends on the CLD model accuracy at the region where the counted spectrum cycles are located. The results shown in Fig. 7 correspond to life predictions for the examined bonded joints loaded under the standardized for wind turbine blades WISPERX spectrum.

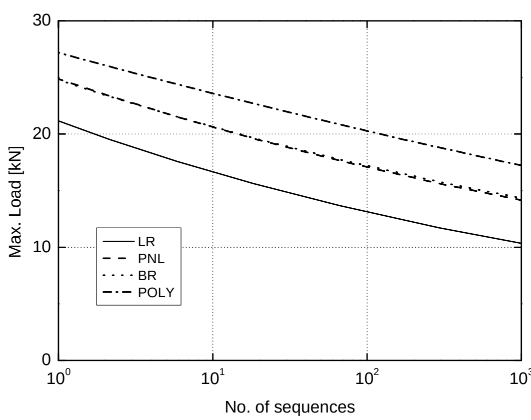

Figure 7. Variable amplitude fatigue life prediction based on the different CLD formulations.

5. Conclusions

The *R*-ratio effect on the fatigue behavior of adhesively-bonded pultruded GFRP double-lap joints was experimentally investigated under different loading conditions. The results showed the high dependency of the fatigue strength on the mean load and therefore the necessity of appropriate modeling of this effect to avoid extensive experimental programs.

In general, the increase of the mean load under constant amplitude loading led to an increase of the tensile and compressive fatigue life of the examined joints. The slopes of the S-N curves were decreased by increasing the mean load level.

Due to the different exhibited failure modes under tension and compression, the CLD derived for the examined bonded joints was asymmetric and shifted toward the compressive domain. This shift was found to be consistent with the higher fatigue strength of joints under compressive loading.

The applicability of several CLD formulations was evaluated for modeling the mean load effect on the constant and the variable amplitude fatigue life. Although accurate predictions were obtained by some of the applied models, the overall accuracy was not consistent under different loading conditions, especially under *R*-ratios around 1. Consequently, different life prediction results emerge after the employment of different CLD formulations.

Acknowledgements

This work was supported by the Swiss National Science Foundation (Grant No 200020-121756), Fiberline Composites A/S, Denmark (supplier of the pultruded laminates), and Sika AG, Zurich (adhesive supplier).

References

[1] Philippidis T.P., Vassilopoulos A.P. Complex stress state effect on fatigue life of GRP laminates. Part I, experimental. *Int J Fatigue*, **24**(8), pp. 813-823 (2002).

[2] Mandell J.F., Samborsky D.D. DOE/MSU composite material fatigue database. Sandia National Laboratories, SAND97-3002. v. 19; 31st March 2010

[3] Kawai M, Koizumi M. Non-linear constant fatigue life diagrams for carbon/epoxy laminates at room temperature, *Compos Part A,* **38**(11), pp. 2342–2353 (2007).

[4] Vassilopoulos A.P., Manshadi B.D., Keller T. Influence of the constant life diagram formulation on the fatigue life prediction of composite materials. *Int J. Fatigue*, **32**(4), pp. 659-669 (2010).

[5] Silverio Freire R.C., Dória Neto A.D., De Aquino E.M.F.. Comparative study between ANN models and conventional equation in the analysis of fatigue failure of GFRP. *Int J Fatigue*, **31**(5), pp. 831–839 (2009).

[6] Hahn H.T. Fatigue behavior and life prediction of composite laminates, in: "*Composite Materials: Testing and Design (Fifth Conference), ASTM STP 674*" edited by Tsai S.W., American Society for Testing and Materials, Philadelphia, pp. 383–417 (1979).

[7] Vassilopoulos A.P. Introduction to fatigue life prediction of composite materials and structures: past, present and future prospects. In: "*Fatigue life prediction of composites and composite structures*" edited by Vassilopoulos A.P, Woodhead Publishing Ltd, Oxford, pp. 1–44 (2010).

[8] Mallick P.K., Zhou Y. Effect of mean stress on the stress-controlled fatigue of a short E-glass fiber reinforced polyamide–6.6. *Int J Fatigue*, **26**(9), pp. 941–946 (2004).

[9] Crocombe A.D., Richardson G. Assessing stress and mean load effects on the fatigue response of adhesively bonded joints. *Int J Adhes Adhes*, **19**(1), pp. 19–27 (1999).

[10] Sarfaraz R, Vassilopoulos A.P., Keller T. Experimental investigation of the fatigue behavior of adhesively-bonded pultruded GFRP joints under different load ratios. *Int J Fatigue*, **33**(11), pp. 1451–1460 (2011).

[11] Vassilopoulos A. P, Manshadi B.D., Keller T. Piecewise non-linear constant life diagram formulation for FRP composite materials. *Int J Fatigue*, **32**(10), pp. 1731–1738 (2010).

[12] Sarfaraz R, Vassilopoulos A.P., Keller T. Experimental investigation and modeling of mean load effect on fatigue behavior of adhesively-bonded pultruded GFRP joints. *Int J Fatigue*, in press (2012), doi: 10.1016/j.ijfatigue.2012.04.021.